Proceedings of *The Riddle of Cooling Flows in Galaxies and Clusters of Galaxies*
May 31 – June 4, 2003, Charlottesville, Virginia, USA
Ed. T. H. Reiprich, J. C. Kempner, & N. Soker

High Resolution X-ray Spectroscopic Constraints on Cooling-Flow Models

John R. Peterson,[1] Steven M. Kahn,[1] Frits B. S. Paerels,[1] Jelle S. Kaastra,[2] Takayuki Tamura,[2] Johan A. M. Bleeker,[2] Carlo Ferrigno,[2] and J. Garrett Jernigan[3]

[1] *Columbia Astrophysics Laboratory, Columbia University, 550 W 120th St., NY, NY 10027, USA*
[2] *SRON National Institute for Space Research, Sorbonnelaan 2, 3584 CA Utrecht, The Netherlands*
[3] *Space Sciences Laboratory, University of California, Berkeley, CA 94720, USA*

arXiv:astro-ph/0310008v1 30 Sep 2003

We present XMM-Newton Reflection Grating Spectrometer observations of X-ray clusters and groups of galaxies. We demonstrate the failure of the standard cooling-flow model to describe the soft X-ray spectrum of clusters of galaxies. We also emphasize several new developments in the study of the soft X-ray spectrum of cooling flows. Although there is some uncertainty in the expected mass deposition rate for any individual cluster, we show that high resolution RGS spectra robustly demonstrate that the expected line emission from the isobaric cooling-flow model is absent below 1/3 of the background temperature rather than below a fixed temperature in all clusters. Furthermore, we demonstrate that the best-resolved cluster spectra are inconsistent with the predicted shape of the differential luminosity distribution and the measured distribution is tilted to higher temperatures. These observations create several fine-tuning challenges for current theoretical explanations for the soft X-ray cooling-flow problem. Comparisons between these observations and other X-ray measurements are discussed.

1. The Cooling-Flow Model

A long-standing theoretical prediction is that the intracluster medium in the cores of galaxy clusters should cool by emitting X-rays in less than a Hubble time (Fabian & Nulsen 1977; Cowie & Binney 1977; Mathews & Bregman 1978). If the cooling proceeds inhomogenously (Nulsen 1986; Johnstone et al. 1992), a range of temperatures is likely to exist in the cooling plasma. Straightforward thermodynamic arguments show that at constant pressure the particular distribution of plasma temperatures is described by the differential luminosity distribution,

$$\frac{dL}{dT} = \frac{5}{2} k \frac{\dot{M}}{\mu m_p} \tag{1}$$

where k is Boltzmann's constant, μm_p is the mean mass per particle, and $\dot{M}$ is the mass deposition rate. This yields a *unique* X-ray spectrum for an assumed set of elemental abundances and a given maximum temperature where the cooling is assumed to begin. Inhomogenous cooling of this sort is broadly called a *cooling flow*.

We can apply Equation 1 to the X-ray spectrum by using standard plasma codes to predict the energy-dependent luminosity at a given temperature. There are three major assumptions: First, it is normally assumed that the total luminosity emitted from the high temperature plasma is not substantially different than that observed in X-rays. If this were not true or if the plasma was indirectly transfering its thermal energy to another source, then this would invalidate the model. Second, we assume that there is no substantial heating that would modify the thermodynamic history of the plasma. Third, we assume that the bulk of the cooling volume is approximately in a steady-state, so that the cooling flow is not dramatically changing during a characteristic cooling time. Although many modifications and theoretical challenges to this simple model have been discussed for more than 25 years, it was not known until recently if the X-ray spectrum deviated significantly from this simple cooling-flow model.

In order to measure a differential luminosity distribution at keV temperatures like that in Equation 1, emission lines from individual ions need to be measured. In particular, it is important to measure emission lines from the Fe L series, which are ions that happen to have their ionization potentials in the temperature range near and below cluster virial temperatures. This is shown in Figure 1 where the relative charge state abundance (elemental abundance times fractional ionic abundance) of various ions is plotted. However, measuring the relative strength of emission from individual Fe L ions is only possible to do in detail with resolving powers ($\frac{\lambda}{\Delta\lambda}$) above 100. These resolving powers are not achievable with non-dispersive CCD experiments like ASCA/SIS, XMM-Newton/EPIC, and Chandra/ACIS, although some information can be obtained from the shape of the unresolved Fe L emission line complex. The Reflection Grating Spectrometer (RGS) on XMM-Newton, however, is capable of high-resolution spectroscopy for sources with spatial extent similar to many cooling flows.

The RGS is a dispersive spectrometer that contains a grating array that is placed behind the XMM mirrors. The grating array deflects photons to a CCD bench. The

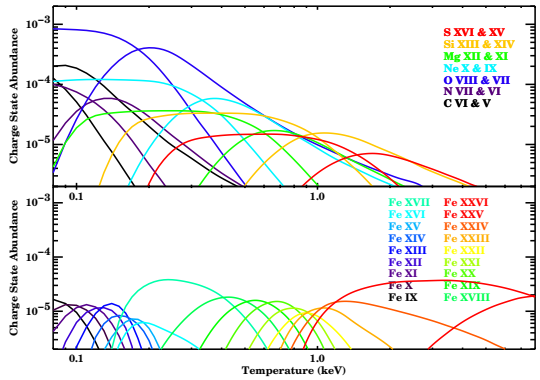

FIG. 1.— Fractional abundance of a given ion plotted against temperature in keV (taken from Arnaud & Raymond 1992). The fractional abundance is multiplied by the abundance of that element relative to hydrogen in the solar neighborhood (Anders & Grevesse 1989). The top plot shows the helium and hydrogen-like charge states for several elements. The bottom plot shows a number of charge states of iron.

RGS was designed to have a relatively high dispersion of 3 degrees for the soft X-ray band in order to compensate for the fact that the XMM mirrors would blur sources by about 10 arcseconds (Kahn & Hettrick 1985). Cooling flows happen to have a similar size to the XMM blurring, so that observations of cooling flows also benefit from the large dispersion angles. The dispersion of an incident X-ray is determined by both the wavelength of the photon and the angle it hits the grating array. Therefore, for a source with significant spatial extent like a cluster, the coupling of the sky position with the wavelength has to be modeled. A Monte Carlo approach has therefore been used to analyze extended source RGS observations. Some discussion of this can be found in Peterson, Jernigan & Kahn (2003a).

2. Spectroscopic Constraints on Cooling Flows

The initial application of the standard cooling-flow model to a high resolution spectrum of a cluster of galaxies is shown in Figure 2. The top panel shows the spectral prediction for a model based on Equation 1. The second panel shows the comparison between the model (blue) and the spectrum of Abell 1835 (red). Notably absent in the data are Fe XVII lines. Finally, the bottom panel shows a model where the emission below 3 keV is suppressed. This fairly simple model of the X-ray emission seems to describe the data quite well. The plasma appears to match the cooling flow model betwen 3 keV and the maximum cluster temperature of 8 keV but not below 3 keV. The obvious theoretical question is why it appears close to matching the cooling flow model at high temperatures, but not at low temperatures. It is clearly not an isothermal spectrum, but it is also inconsistent with a complete cooling flow model. Full details of this comparison can be found in Peterson et al. (2001). Other grating observations contain similar results (Tamura et al. 2001a; Kaastra et al. 2001; Tamura et al. 2001b; Xu et al. 2002; Sakelliou et al. 2002).

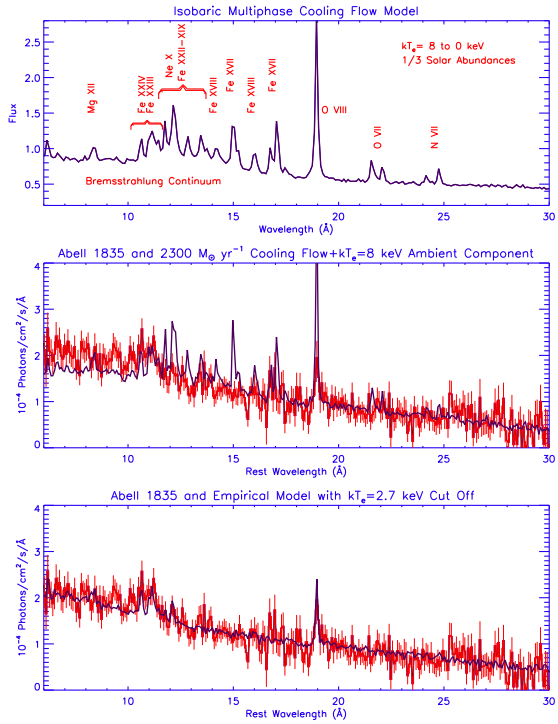

FIG. 2.— Comparison of the cooling flow model to Abell 1835. The top panel shows the cooling flow model based on Equation 1 in the text. Note the numerous Fe L lines predicted in the 10 to 17 Å region. The middle panel shows the comparison of that model with the data from the galaxy cluster Abell 1835 which was thought to host a massive cooling flow. The bottom panel shows the cooling flow model with the emission suppressed below 3 keV.

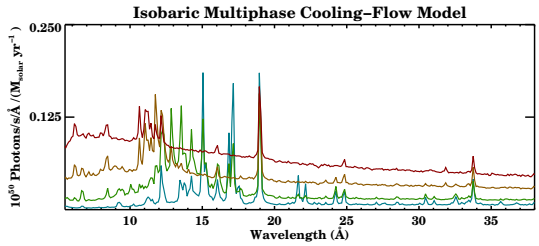

FIG. 3.— The emission spectrum of the standard cooling flow model broken up into several temperature bins. The red line shows the 3 to 6 keV spectrum, the yellow shows the 1.5 to 3 keV spectrum, the green shows the 0.75 to 1.5 keV spectrum and the blue shows the 0.375 to 0.75 keV spectrum. The normalization of each of the components is adjusted to see where the cooling flow model fails.

If we decompose the spectrum in the top panel in Figure 2 into different temperature ranges, we arrive at the spectra in Figure 3. Here we plot the 6 to 3 keV (red), 3 to 1.5 keV (yellow), 1.5 to 0.75 keV (green), and 0.75 to 0.375 keV spectrum (blue). Then if we fit the observed X-ray spectra while allowing the relative normalization of each of these four spectra to vary, we can fit the X-ray spectra of 14 cooling-flow clusters of galaxies quite well. This is shown in the spectral fits in Figures 4-6. These fits also use a spatial model for the cluster emission folded through the Monte Carlo for the RGS. The red line shows the fit, the blue histogram is the data, and the green line is the standard cooling flow model with no adjustments.

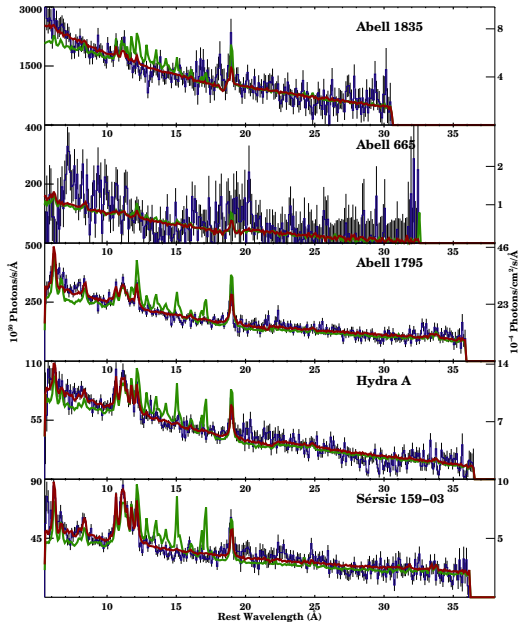

FIG. 4.— Fluxed spectra of several hot (about 5 keV) clusters of galaxies. The red line is an empirical fit allow the normalization of the cooling flow model for several temperature ranges to be adjusted. The green line is the standard cooling flow model with no adjustments. The model fails most strongly from Fe XVII lines, which implies that the lowest temperature emission is absent.

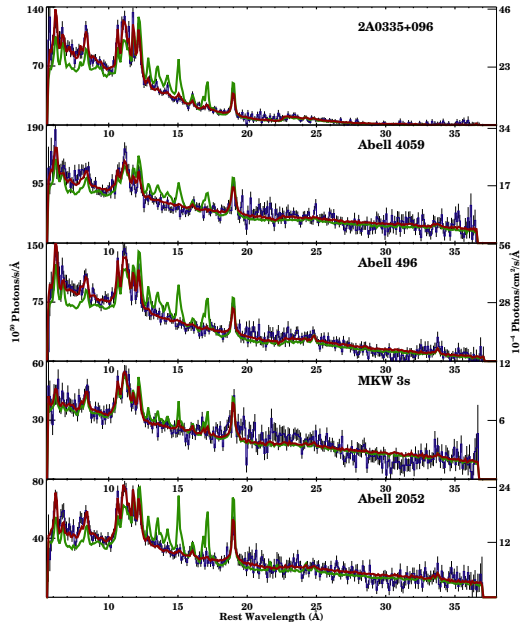

FIG. 5.— The same plot as Figure 4 but with medium temperature (3 to 5 keV) clusters.

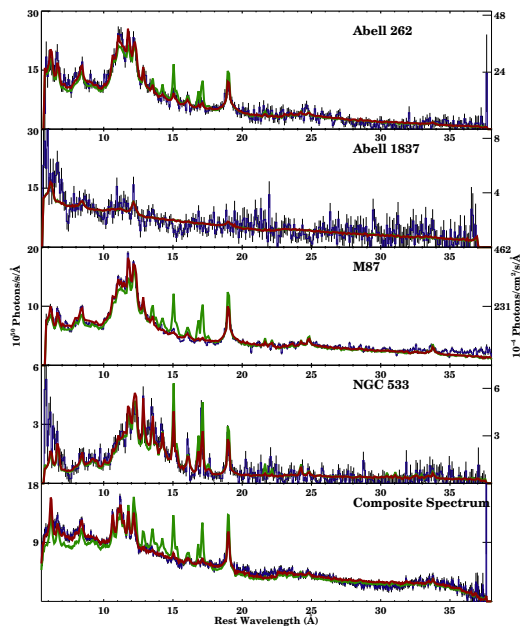

FIG. 6.— The same plot as Figure 4 and 5 but with cool (less than 3 keV) clusters and groups.

The cooling flow model deviates significantly from the data in a similar manner to the Abell 1835 comparison in Figure 2. The low temperature emission is not present or significantly reduced in the cluster spectra. Full details of the model and analysis method can be found in Peterson et al. (2003b).

Figure 7 shows the differential luminosity of each of the four spectra (proportional to the total normalization given by the fit) against the temperature. Each cluster is shown in a different color and the actual detections are connected by a line. If the cooling flow model were correct, then the points should line close to the line $y = 1$. Figure 8 shows the same plot but it is plotted against the temperature relative to the maximum temperature. The points appear roughly consistent with a power law in fractional temperature where the index is near 1 to 2.

Figure 7 and 8 demonstrate several aspects of the failure of the cooling-flow model. First, it is clear that significant quantities of plasma below the maximum temperature always exists. Second, the model appears to fail at a fraction of the maximum temperature rather than a fixed value as shown by the luminosity distribution crossing the line $y = 1$ near $T = \frac{1}{3}$ in Figure 8. Furthermore, the model fails in its shape (it is not horizontal) since it is tilted towards higher temperatures and the normalization at low temperatures is not the only discrepancy. The overall normalization, however, is somewhat difficult to interpret in the absence of a new theoretical model, since a new model would probably add or subtract heat to the system which affects the normalization. There is also significant scatter in both plots. It is not clear whether this is due to subtle fitting degeneracies or is a real difference between cooling flows. We also cannot be certain if the empirical model, the power law in fractional temperature, continues to arbitrarily low temperatures. It is clear, however, that the model is off by as much as an order of magnitude at the lowest temperatures. Finally, it appears that the simple temperature cut-off model used in Figure 2 might be oversimplified. The best-resolved

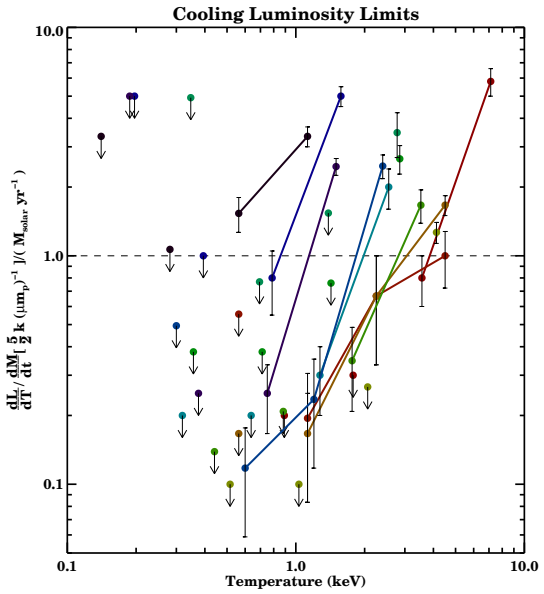

FIG. 7.— A comparison of the luminosity in specific temperature ranges to the cooling flow model. See the text for details.

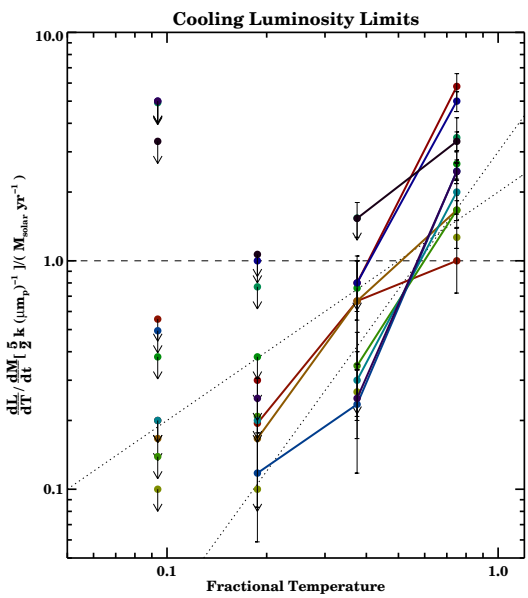

FIG. 8.— Same as Figure 7 but plotted as a function of the fraction of the maximum temperature.

spectra like that for 2A0335+096 has emission lines from Fe XXIV through XVIII. This has forced us to use a more complex model than the cut-off model to match the lowest temperature emission. Similarly, just reducing the overall normalization and therefore the implied mass deposition, $\dot{M}$, also does not describe these observations. Clearly, the many aspects of these observations should offer some clue to the solution to this problem.

3. Theoretical Challenges

There are many ideas for possible mechanisms which would either add or subtract heat from cooling flows (see e.g., Peterson et al. 2001; Fabian et al. 2001; Böhringer et al. 2002; Sasaki & Yamasaki 2002; Makishima et al. 2001; Peterson et al. 2003b; Mathews & Brighenti 2003). Promising scenarios are documented in these proceedings and include dust cooling (Fabian et al. 2001; Mathews & Brighenti 2003), cold cloud interface mixing (Begelman & Fabian 1990; Fabian et al. 2001), interactions with cosmic rays (Gitti, Brunetti, & Setti 2002), heating through processes associated with relativistic AGN outflows (Rosner & Tucker 1989; Binney & Tabor 1995; Churazov et al. 2001; Brüggen & Kaiser 2001; Quilis 2001; David et al. 2001; Nulsen 2002; Kaiser & Binney 2002; Ruszkowski & Begelman 2002; Soker & David 2003; Brighenti & Mathews 2003), cluster merging (Markevitch et al. 2001), or significant heat transfer between the outer region and cores of clusters (Tucker & Rosner 1983; Stewart et al. 1984; Zakamska & Narayan 2001; Voigt et al. 2002; Fabian, Voigt, & Morris 2002; Soker 2003). Less interesting explanations that might involve subtle errors in the application of Equation 1, such as a gross error in the plasma codes, are probably not relevant. This is likely not to be the case since some cataclysmic variables are observed to have X-ray spectra almost exactly like that in the top panel in Figure 2 (Mukai et al. 2003). This is understood by the idea that the accretion of material from the secondary to the white dwarf where it must cool down to the photospheric temperature essentially proceeds the same way as a classic cooling flow.

Generally, there are three major requirements for any successful model. First, the average heating or additional cooling power should be comparable to the X-ray luminosity from cooling flows. Most calculations have shown that this could be true for a number of different models. The second and somewhat more confusing requirement is that the mechanism should work more effectively at lower temperatures or should begin to operate right before complete cooling occurs. The isobaric cooling time is proportional approximately to the second power of temperature. So if the cooling starts to be disrupted characteristically at $\frac{1}{3}$ of the maximum temperature, why does it stop when it is $\frac{8}{9}$ of the way to completion? Finally, a successful model must also add or subtract the heat at the right time at all spatial positions. The observed spatial distribution of the X-ray emission, however, is somewhat complicated as we discuss in the following section. The global problem, however, is quite clear– the X-rays from the lowest temperatures are not present in the entire cooling flow volume.

4. Comparison with other X-ray observations

Some discussion on the nature of fitting spatially-resolved collisional X-ray spectra is warranted, since the comparison of these observations with those derived from other X-ray instruments can be complicated and was under frequent discussion at this conference. If the ICM is optically-thin to its own radiation and is in collisional equilibrium then its differential luminosity distribution is described by two functions,

$$\frac{d^2L}{dTd\Omega} = f_1(T,\Omega) \quad (2)$$

$$\frac{dA_i}{d\Omega} = f_2(\Omega) \quad (3)$$

where the first function f_1 describes the differential luminosity distribution as a function of temperature, T, at each solid angle element $d\Omega$ and the second function f_2 specifies an abundance map for each element. The measurement of other quantities, such as a density or volume, are always indirectly derived from these two functions. Note also that the function, $\frac{d^2A_i}{dTd\Omega}$, is not actually observable in practice. This is because a plasma consisting of multiple temperatures will emit line emission that can be separately measured from each temperature region but the continuum emission from each temperature region will just contribute to one overall continuum. Even if the plasma were divided into different temperatures each with their own metallicity, only one overall metallicity can be measured for any one spectrum.

The ability to measure a temperature distribution, $\frac{dL}{dT}$, is determined by the number of counts in the spectrum, the resolution of the instrument, and fundamental atomic physics issues. For a high resolution spectrum with a large number of counts, the X-ray temperature distribution probably cannot be divided into much more than 8 or so temperature bins. This is because there are only so many strong emitting X-ray ions. The Fe K and L series, for example, have 10, but their overlap in specific temperatures ranges makes disentangling the temperature distribution in great detail difficult. Line ratios between emission lines from the same ion are only weakly temperature sensitive for the normal temperature ranges that the ion is produced.

With a typical RGS cluster observation of about 30,000 source photons, we have typically found that deviding the X-ray temperature range into 4 logarithmic bins usually provides a robust solution. With more photons, we expect that a slightly more detailed analyses can be performed. With the non-dispersive CCD instruments of EPIC and Chandra less information can be extracted. Individual X-ray ions are not detected precisely, but their emission is blended significantly. It appears that usually determining much more than two temperatures (or two temperature ranges) is extremely difficult without a very large number of counts.

The RGS observations place a different set of constraints on the spatial distribution of the luminosity distribution, $\frac{dL}{d\Omega}$ than EPIC or Chandra observations. The ability to do this, of course, depends on the spatial resolution of the instrument provided enough X-ray photons are collected. Therefore, Chandra can constrain the angular luminosity distribution at the arcsecond scale, whereas EPIC can constrain the distribution at the several arcsecond scale. RGS observations can utilize the cross-dispersion information (the distance photons are detected perpendicular to the dispersion axis of the spectrometer) to measure the spatial distribution almost as good as the EPIC resolution. The shapes of line profiles at least in principle can constrain the distribution in the dispersion direction.

The ability to measure the total two-dimensional function, $\frac{d^2L}{dTd\Omega}$ is obviously complicated and probably is different for every observation of every cluster. We may have to guess at what the true distribution or what the shape of this function is for cooling flows. Making conclusive statements about isothermality or a preferred formulation of the temperature distribution is very challenging and depends heavily on the capabilities of that instrument. All of the instruments, however, have generally shown an average temperature decline. The RGS observations presented here show evidence for a steep differential luminosity distribution of order T^1 or T^2 if averaged over the entire cooling flow. The deepest EPIC observations show steep multiphase distributions (possibly power laws with indices greater than T^2) with overall temperature contrasts that are probably greater than a factor of two (Kaastra et al. 2003; Lewis et al. 2003). Chandra thermal images have shown non-spherical temperature variations at levels less than 50 % (Sanders & Fabian 2003). We might speculate that all the observations have given us a picture that the combination of an overall temperature decline and a steep multiphase distribution (T^3) at each radius combines to give an overall differential distribution near to what has been measured with the RGS (T^1 or T^2). This, however, has not been fully explored nor is it clear how much difference there is between any of the clusters.

The abundance map, $\frac{dA_i}{d\Omega}$, is only beginning to be measured since it depends heavily on getting the temperature distribution correct. Furthermore, deviations from collisional equilbrium have yet to be fully explored. In addition, the optically-thin assumption as well could be violated by resonant scattering but the effect is either observationally controversial (see e.g., Böhringer et al. 2002; Xu et al. 2002; Churazov et al. 2003) or could be different for every cluster due to varying velocity fields.

5. **Future Work**

As we have argued in the previous section, there is much more work to be done in clarifying the observational situation in X-rays. Similarly, the connection of these observations to other wavelengths is very incomplete. In particular, maps that correlate the quantity of missing X-rays with the detections of cold material will be important (Edge et al. 2002; Edge & Frayer 2003). Theoretical studies should continue to build towards a final solution.

It has been previously discussed that cooling flows of some form are necessary to cool galaxies to form stars before they get incorporated into much larger structures (White & Rees 1978). Unless the solution to the soft X-ray cooling flow problem is endemic to cluster scales, it could have far-reaching consequences for structure formation.

JRP would like to thank the conference organizers and the attendees for a very successful conference. Work on the RGS at Columbia University and U. C. Berkeley is

supported by NASA. The laboratory for Space Research, Utrecht is supported by NWO, the Netherlands Organization for Scientific Research.

References

Anders, E. & Grevesse, N. 1989, Geochimica et Cosmochimica Acta 53, 197.
Arnaud, M. and J. Raymond, 1992, ApJ 398, 394.
Begelman, M. & Fabian, A. C. 1990, MNRAS 244, 26.
Binney, J. & Tabor, G. 1995, MNRAS 276, 663.
Böhringer, H., Matsushita, K., Churazov, E., Ikebe, Y., & Chen, Y. 2002, A&A 382, 804.
Brighenti, F. & Mathews, W. G. 2003, ApJ 587, 580.
Brüggen, M. & Kaiser, C. R. 2001, MNRAS 325, 676.
Churazov, E., Sunyaev, R., Forman, W., Böhringer, H. 2001, ApJ 554, 261.
Churazov, E., Forman, W., Jones, C., Sunyaev, R., & Böhringer, H. 2003, MNRAS submitted.
Cowie, L. L. & Binney, J. 1977, ApJ 215, 723.
David, L. P., Nulsen, P. E. J., McNamara, B. R., Forman, W., Jones, C., Ponman, T., Robertson, B., & Wise, M. 2001, ApJ 557, 546.
Edge, A. C. & Frayer, D. T. 2003, ApJ 594, 13.
Edge, A. C. et al. 2002, MNRAS 337, 49.
Fabian, A. C., Voigt, L. M., & Morris, R. G. 2002, MNRAS 335, L71.
Fabian, A. C., Mushotzky, R. F., Nulsen, P. E. J., & Peterson, J. R. 2001, MNRAS 320, 20.
Fabian, A. C. & Nulsen, P. E. J. 1977, MNRAS 180, 479.
Gitti, M., Brunetti, G., & Setti, G., A&A 386, 456.
Johnstone, R. M., Fabian, A. C., Edge, A. C., & Thomas, P. A. 1992, MNRAS 255, 431-440.
Kaastra, J. S. et al., this conference.
Kaastra, J. S., Ferrigno, C., Tamura, T., Paerels, F. B. S., Peterson, J. R., & Mittaz, J. P. D. 2001, A & A 365, 99.
Kaiser, C. & Binney, J. 2002, MNRAS 338, 837.
Kahn, S. M. & Hettrick, M. C. 1985, in ESA Proceedings of a ESA Workshop for a Cosmic X-ray Spectroscopy Mission, Paris: ESA, 237.
Lewis, A. D., Buote, D. A., Mathews, W. G., & Brighenti, F. 2003, this conference.
Makishima, K. et al. 2001, PASJ 53, 401.
Markevitch, M., Vikhlinin, A., & Mazzotta, P., 2001, ApJ 562, L153.
Mathews, W. G. & Bregman, J. N. 1978, ApJ 224, 308.
Mathews, W. G. & Brighenti, F. 2003, ApJ 590, 5.
Mukai, K., Kinkhabwala, A., Peterson, J. R., Kahn, S. M, & Paerels, F. B. S. 2003, ApJL 586, 77.
Nulsen, P. E. J., David, L. P., McNamara, B. R., Jones, C., Forman, W. R., Wise, M. 2002, ApJ 568, 163.
Nulsen, P. E. J. 1986, MNRAS 221, 377.
Peterson, J. R. et al. 2003a, ApJ 590, 207.
Peterson, J. R., Jernigan, J. G. & Kahn, S. M. 2003b, Proc. SPIE 4847.
Peterson, J. R. et al. 2001a, A & A 365, 104.
Quilis, V., Bower, R. G., & Balogh, M. L. 2001, MNRAS 328, 1091.
Rosner, R. & Tucker, W. 1989, ApJ 338, 761.
Ruszkowski, M. & Begelman, M. C. 2002, ApJ 586, 384.
Sakelliou, I. et al., A & A 391, 2002.
Sanders, J. S. & Fabian, A. C. 2003, this conference.
Sasaki, S. & Yamasaki, Y. 2002, PASJ 54, 1.
Soker, N. 2003, MNRAS 342, 463.
Soker, N. & David, L. P. 2003, ApJ 589, 77.
Stewart, G. C., Fabian, A. C., Nulsen, P. E. J., & Canizares, C. R. 1984, ApJ 278, 536.
Tamura, T. et al. 2001, A & A 365, 87.
Tamura, T., Bleeker, J. A. M., Kaastra, J. S., Ferrigno, C., & Molendi, S. 2001, A & A 379, 101.
Tucker, W. H. & Rosner, R. 1983, ApJ 267, 547.
Voigt, L. M., Schmidt, R. W., Fabian, A. C., Allen, S. W. & Johnstone, R. M. 2002, MNRAS 355, 7.
White, S. D. M. & Rees, M. J. 1978, MNRAS 189, 341.
Xu, H. et al. 2002, ApJ 576, 600.
Zakamska, N. & Narayan, R. 2002, ApJ 582, 162.